

First principles study of behavior of helium at Fe(110)-graphene interface

Yan-Mei Jing(荆艳梅) and Shao-Song Huang(黄绍松)
Citation: Chin. Phys. B, 2021, 30 (**4**): 046802. DOI: 10.1088/1674-1056/abd46d
Journal homepage: http://cpb.iphy.ac.cn; http://iopscience.iop.org/cpb

What follows is a list of articles you may be interested in

Preparation of AlN film grown on sputter-deposited and annealed AlN buffer layer via HVPE

Di-Di Li(李迪迪), Jing-Jing Chen(陈晶晶), Xu-Jun Su(苏旭军), Jun Huang(黄俊), Mu-Tong Niu(牛牧童), Jin-Tong Xu(许金通), and Ke Xu(徐科)
Chin. Phys. B, 2021, 30 (**3**): 036801. DOI: 10.1088/1674-1056/abd392

Interfaces between MoO_x and MoX_2 (X = S, Se, and Te)

Fengming Chen(陈凤鸣), Jinxin Liu(刘金鑫), Xiaoming Zheng(郑晓明), Longhui Liu(刘龙慧), Haipeng Xie(谢海鹏), Fei Song(宋飞), Yongli Gao(高永立), and Han Huang(黄寒)
Chin. Phys. B, 2020, 29 (**11**): 116802. DOI: 10.1088/1674-1056/abb310

Covalent coupling of DNA bases with graphene nanoribbon electrodes: Negative differential resistance, rectifying, and thermoelectric performance

Peng-Peng Zhang(张鹏鹏), Shi-Hua Tan(谭仕华)†, Xiao-Fang Peng(彭小芳)‡, and Meng-Qiu Long(龙孟秋)
Chin. Phys. B, 2020, 29 (**10**): 106801. DOI: 10.1088/1674-1056/aba9bf

PEALD-deposited crystalline GaN films on Si (100) substrates with sharp interfaces

San-Jie Liu(刘三姐), Ying-Feng He(何荧峰), Hui-Yun Wei(卫会云), Peng Qiu(仇鹏), Yi-Meng Song(宋祎萌), Yun-Lai An(安运来), Abdul Rehman(阿布度-拉赫曼), Ming-Zeng Peng(彭铭曾), Xin-He Zheng(郑新和)
Chin. Phys. B, 2019, 28 (**2**): 026801. DOI: 10.1088/1674-1056/28/2/026801

Analysis of meniscus beneath metastable droplets and wetting transition on micro/nano textured surfaces

Yanjie Li(李艳杰), Xiangqin Li(李香琴), Tianqing Liu(刘天庆), Weiguo Song(宋伟国)
Chin. Phys. B, 2018, 27 (**8**): 086801. DOI: 10.1088/1674-1056/27/8/086801

First principles study of behavior of helium at Fe(110)–graphene interface*

Yan-Mei Jing(荆艳梅) and Shao-Song Huang(黄绍松)†

Key Laboratory of Material Modification by Laser, Ion and Electron Beams (Dalian University of Technology), Ministry of Education, Dalian 116024, *China*

(Received 18 August 2020; revised manuscript received 11 December 2020; accepted manuscript online 17 December 2020)

Recently, metal–graphene nanocomposite system has aroused much interest due to its radiation tolerance behavior. However, the related atomic mechanism for the metal–graphene interface is still unknown. Further, stainless steels with Fe as main matrix are widely used in nuclear systems. Therefore, in this study, the atomic behaviors of point defects and helium (He) atoms at the Fe(110)–graphene interface are investigated systematically by first principles calculations. The results indicate that graphene interacts strongly with the Fe(110) substrate. In comparison with those of the original graphene and bulk Fe, the formation energy values of C vacancies and Fe point defects decrease significantly for Fe(110)–graphene. However, as He atoms have a high migration barrier and large binding energy at the interface, they are trapped at the interface once they enter into it. These theoretical results suggest that the Fe(110)–graphene interface acts as a strong sink that traps defects, suggesting the potential usage of steel–graphene with multiply interface structures for tolerating the radiation damage.

Keywords: Fe(110)–graphene, helium, interface, first principles calculations

PACS: 68.55.Ln, 68.65.Pq **DOI:** 10.1088/1674-1056/abd46d

1. Introduction

With the rapid development of advanced nuclear energy systems, the need for the development and application of structural materials with higher radiation tolerance has increased.[1] Point defects (vacancies and interstitials) generated by high-energy neutrons can evolve into extended defects such as voids and interstitial clusters within the structural materials at elevated temperatures. In addition, a certain number of helium (He) are produced by the (n, α) transmutation reaction.[2] Owing to the low solubility of He atoms, their diffusion and aggregation results in the precipitation and nucleation of He bubbles.[3] The synergistic interaction of these defects leads the mechanical properties of the structural material to degrade.[4–10] Increasing the fraction of interface/boundaries in materials is an important strategy to enhance the irradiation effect tolerance by providing more defect recommendation sites.[11–14] In particular, multilayer metallic systems such as W/Cu,[15] Cu/Nb,[16] and Cu/V[17] systems have been studied extensively as structural materials for mitigating radiation damage.

Further, graphene has attracted much attention due to its highly dense interface,[18–20] with a two-dimensional structure packed by a single layer of C atoms. Several studies reported their results on the radiation damage resistance of copper–graphene, nickel–graphene, and vanadium–graphene nanocomposites through molecular dynamics and experiments,[21–23] it was found that the metal–graphene nanocomposite had less defects remaining in the bulk region after collision cascades, illustrating the self-healing performance. However, the atomic mechanism was still unknown, especially for the interaction between the graphene and metal substrates. Furthermore, as is well known, stainless steels, in which Fe is the basic element in the matrix (with more than 80 wt%), are the most commonly constructive and prospective materials in nuclear systems. As stated, He is an important product of neutron transmutation, affecting many of the properties of structural materials with point defects.[24–29] Thus, previous studies promoted us to figure out whether the Fe–graphene interface can affect the behaviors of intrinsic defects and act as a good He permeation barrier. In this study, we aim to investigate the potential usage of steel–graphene with multiply interface structures for tolerating the radiation damage. Therefore, using *ab initio* calculations, we investigate the energetical stability of the Fe–graphene system, the formation of the intrinsic defects, and the behaviors of an interstitial He atom. The rest of this paper is organized as follows. The method of first-principles calculations, and calculational equations are presented in Section 2. In Section 3, the results of the behaviors of the intrinsic defects, and He atoms in the Fe(110)–graphene system are discussed. The major findings are summarized in Section 4.

*Project supported by the Nuclear Power Technology Innovation Center Program, National Defense Science & Technology Industry, China (Grant No. HDLCXZX-2019-ZH-028).

†Corresponding author. E-mail: huangss@dlut.edu.cn

© 2021 Chinese Physical Society and IOP Publishing Ltd

2. Computational method

For all computations, we adopt density functional theories (DFT)[30,31] as implemented in the Vienna *Ab initio* Simulation Package (VASP).[32,33] The spin effects are considered in all calculations. The full-potential frozen-core all-electrons projector-augmented wave (PAW) potentials was adopted for the ion–electron interaction. The generalized gradient approximation parameterized by Perdew, Burke, and Ernzerhof (GGA-PBE) was used to describe the exchange-correction interaction.[34–37] The van der Waals (vdW) interactions in layered materials were corrected by using the Grimme's semiempirical DFT-D3 scheme.[38] The cutoff energy was set to be 400 eV. The Brillouin zones of the supercells were sampled with $3\times3\times1$ uniform $\boldsymbol{k}$ points mesh. The supercell was fully optimized by fixing the cell parameters through using the convergence criterion of 10^{-4} eV for the electronic energy and 10^{-2} eV/Å for forces acting on each atom. The Fe(110) surface was regarded as a good candidate structure for a new type of graphene nanopatterning due to its distorted hexagonal symmetry.[39] Hence, the supercell consisted of 4×4 graphene and a six-layer slab for the Fe(110) substrate with in-plane lattice vectors of $\boldsymbol{b}_1=4\boldsymbol{a}_1$ and $\boldsymbol{b}_2=-3\boldsymbol{a}_1+4\boldsymbol{a}_2$, where $\boldsymbol{a}_1$ and $\boldsymbol{a}_2$ are the primitive vectors of the Fe(110) surface. The mismatches of the lattice and angles were $\sim3.68\%$ and 5.13%, respectively. The structure was found to be in good consistence with that studied by Pei *et al*.[40] A 15-Å-thick vacuum space was implemented in the vertical direction to minimize the interaction between adjacent image cells. In the first step of relaxation, the C atoms were allowed to relax only along the Z axis. After convergence, the positions of C and Fe atoms in the three topmost substrate layers were allowed to relax over all the coordinates, while the bottom three Fe layers were fixed to model the structure of bulk Fe. The lattice parameter of graphene was set to be 2.468 Å in conformity with previous studies.[41,42] The lattice parameter of the Fe unit cell was set to be 2.87 Å in agreement with a prior DFT study.[40] The climbing image nudged elastic band (CI-NEB)[43,44] method was adopted to investigate the diffusion of He atoms at the Fe(110)–graphene interface.

The interaction between graphene and the metal substrate can be characterized by the interfacial binding energy (E_b) defined as

$$E_\mathrm{b}=\frac{\left(E_\mathrm{total}-E_\mathrm{sub}-E_\mathrm{g}\right)}{N_\mathrm{c}}, \tag{1}$$

where E_total, E_sub, and E_g are the energy of the composite system, standalone substrate, and graphene, respectively, and N_c is the number of C atoms in the graphene sheet.

The binding energy of two defects, A and B, in the Fe(110)–graphene system is given by[45]

$$E_\mathrm{b}(\mathrm{AB})=E(\mathrm{A})+E(\mathrm{B})-E(\mathrm{AB})-E(\mathrm{perfect}). \tag{2}$$

Here, $E(\mathrm{A})$ or $E(\mathrm{B})$ is the total energy of a single defect in the structure, $E(\mathrm{AB})$ is the total energy of a supercell with two defects, and $E(\mathrm{perfect})$ is the total energy of the prefect structure without any defects. Following this convention, the positive binding energy corresponds to exothermic defect formation reaction, implying an attractive interaction between A and B.

The formation energy of a single vacancy or an interstitial atom (E^f) in the Fe(110)–graphene structure is defined as

$$\begin{aligned}E^\mathrm{f}=&E(\mathrm{defect})+E(\mathrm{perfect})\\&+mE(\mathrm{Fe})+nE(\mathrm{C})+pE(\mathrm{He}),\end{aligned} \tag{3}$$

where $E(\mathrm{defect})$ and $E(\mathrm{perfect})$ are the total energy of the Fe(110)–graphene system with and without a point defect, respectively; $E(\mathrm{Fe})$ represents the cohesive energy per Fe atom in bcc Fe, $E(\mathrm{C})$ denotes the energy per C atom in graphene; $E(\mathrm{He})$ is the energy of an isolated He atom; $m=1$, $n=0$, and $p=0$ for an Fe vacancy in the Fe layer; $m=0$, $n=1$, and $p=0$ for a C vacancy in the graphene layer; $m=-1$, $n=0$, and $p=0$ for an Fe interstitial atom; $m=0$, $n=-1$, and $p=0$ for a C interstitial atom; $m=0$, $n=0$, and $p=-1$ for an He interstitial atom.

3. Results and discussion

3.1. Structure and bonding properties

Figure 1 shows the structure of the Fe(110)–graphene interface; a Moiré pattern forms in the Fe(110)–graphene, with a large corrugation of the graphene layer. Owing to the lattice mismatch between the Fe substrate and graphene, C atoms occupy various adsorption sites on the Fe substrate.[46] The results indicate that the interaction between the Fe substrate and graphene is strong. In this case, it is vital to investigate the equilibrium binding distance and binding energy of the Fe(110)–graphene system. According to the equilibrium binding distance, the interaction between graphene and the substrate can be divided into two classes:[41] one is represented by an equilibrium binding distance, d of ≤2.3 Å which indicates strong interaction or chemisorption, and the other belongs in weak interaction or physisorption. According to Eq. (1), the binding energy of the Fe(110)–graphene structure is 0.05 eV/C and the binding distance is ~2.13 Å while the previously reported experimental and theoretical value are ~2.09 Å and 2.10 Å respectively.[39,47] From the energy and distance viewpoint, the binding between the Fe substrate and graphene is strong. The graphene layer on the Fe(110) substrate exhibits a similar binding behavior to that observed on other metal substrates such as Ni, Co, and Pd.[48–50]

The total density of states (TDOS) of the Fe(110)–graphene system and local density of states (LDOS) between graphene and the topmost Fe layer are shown in Fig. 2. The Fe-d orbital significantly affects the TDOS near the Fermi level. Thus, the metal substrate determines the Fermi level of the composite material. The strong hybridization of the Fe-d state and C-p state in the LDOS indicates that a strong covalent bond forms between the Fe atom and C atom, similar to the previously reported cases of graphene on Rh (111)[51] and Ni (111).[52] The small interfacial distance can result in the overlap of the wave functions of the d electrons of the metal and p electrons of graphene, leading to orbital hybridization.

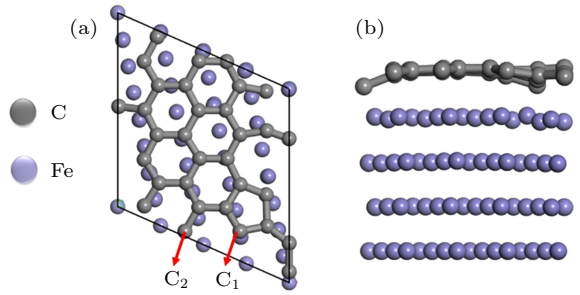


Fig. 1. Structure of Fe(110)–graphene system, showing (a) top view and (b) side view of structure, with purple and gray balls representing Fe atom and C atom, respectively.

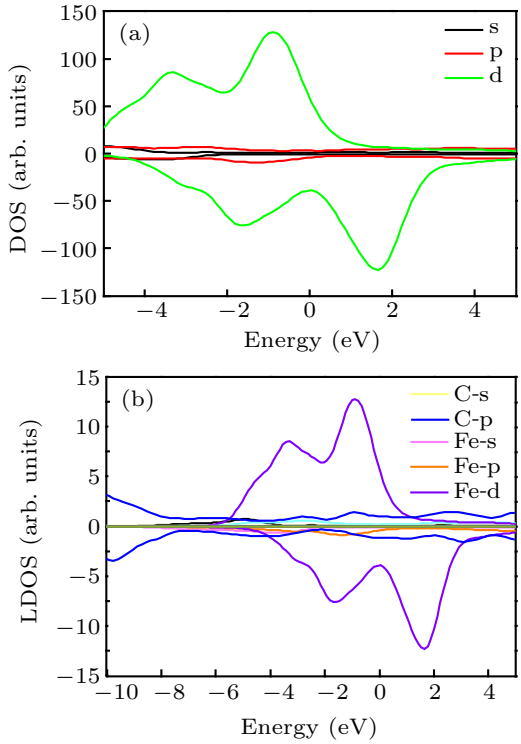


Fig. 2. (a) Total density of states (TDOS) of Fe(110)–graphene system and (b) local density of states (LDOS) between graphene and the topmost Fe layer, with colored solid lines showing projected DOS from s, p, d orbitals, respectively.

For the visualization of the binding between the Fe substrate and graphene, figures 3 and 4 depict the difference between charge densities in the interfacial region. The charges are mainly redistributed at the interface ($\Delta\rho$ zone at 10.43 Å < Z < 12.45 Å. Graphene has two types of C atoms as shown in Fig. 1. Further, figure 3 evidently shows the charges accumulating between the C_1 atom and Fe atom, indicating that the interaction between these atoms is stronger than that between C_2 atom and Fe atom. The interaction between Fe atom and C_1 atom, and the interaction between Fe atom and C_2 atom of graphene are significantly different, and depend on their positions. Thus, the Fe atoms reduce the strength of the C–C bond via charge transfer and orbital hybridization. The redistribution of charges contributes to the formation of covalent Fe–C bonds, which increases the compositing of the Fe substrate and graphene layer.

Weser *et al.*[53] and Dedkov *et al.*[54] reported a magnetic moment of approximately 0.05 μ_B–0.1 μ_B per carbon atom for the C atoms of a graphene layer contacting a ferromagnetic Ni(111) substrate. In this work, the magnetic moment of C_1 was found to be -0.036 μ_B, which forms an antiferromagnetic couple with the nearest Fe atom. On the other hand, the magnetic moment of the C_2 atom was approximately $+0.022$ μ_B. This result is consistent with that reported by Liu *et al.*[47] The magnetic moments of C atoms in Fe(110)–graphene are attributed to the Fe3d–C2p orbital hybridization.

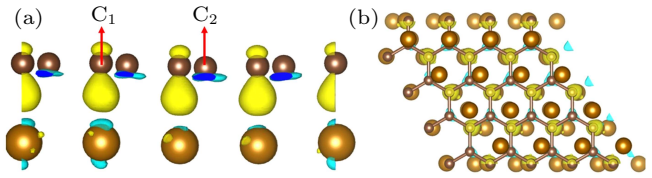


Fig. 3. Differential charge density of Fe(110)–graphene interface region (isovalue: 0.005 e/Å^3), showing (a) side view and (b) top view of interface, where big and small balls represent Fe and C atoms, respectively, blue contour denotes electron depletion region, and yellow contour refers to electron accumulation region.

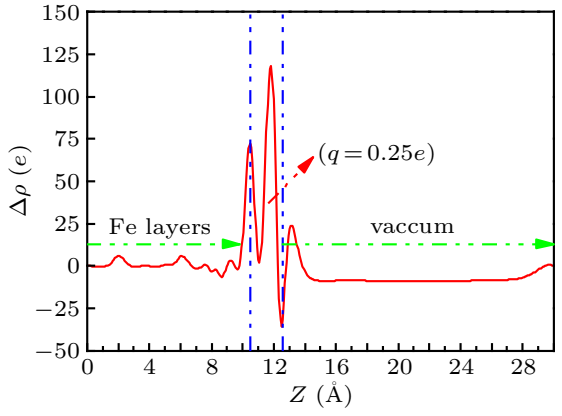


Fig. 4. Interlayer charge difference in Fe(110)–graphene interface region ($\Delta\rho = \rho_{\text{interface}} - \rho_{\text{Fe}} - \rho_{\text{C}}$). Area between red line and 0 line displays the value of electron depletion or accumulation. Value at interface around 10.43 Å < Z < 12.45 Å is positive, indicating electron accumulation.

3.2. Formation and stability of intrinsic defects

The formation energy values of single vacancies of the C and Fe atoms in different layers in Fe(110)–graphene are calculated, and the results are listed in Table 1. The formation

energy of the C vacancy in a single graphene layer is also calculated. The single graphene layer is obtained by removing all the Fe atoms in the Fe(110)–graphene system. That is, the single graphene layer is the same as the graphene layer in the Fe(110)–graphene in terms of the initial size and shape. The C vacancy formation energy in the single graphene layer is 8.09 eV, in agreement with previously calculated results.[55,56] However, it is slightly larger than the experiment value of 7.0 ± 0.5 eV.[15] The C vacancy formation energy values of the two types of C atoms (*i.e.*, C_1 atom and C_2 atom) in Fe(110)–graphene are 1.94 eV and 1.97 eV, respectively, which are lower than those for the single graphene layer. This indicates that the C vacancy prefers to form in Fe(110)–graphene. The result is consistent with that reported for Cu/graphene/Cu.[56] The hybridization of C atoms in graphene changes from sp^2 to sp^3 due to its interaction with the metal. Consequently, the strength of the in-plane C–C bond is weakened.[57] The formation energy of the Fe vacancy increases with the number of Fe layers increasing. The formation energy of the Fe vacancy in the third layer is close to that in bulk Fe (~ 2.17 eV). Hence, it is reasonable for us to fix the three bottom Fe layers. The Fe vacancy formation energy for the topmost layer is lower than those for the other layers and bulk Fe, indicating that Fe vacancies prefer to form at the interface rather than stay in bulk Fe. This phenomenon can be attributed to the fact that the interaction between Fe and graphene is weaker than the binding of Fe–Fe in bulk Fe.

Table 1. Formation energy values of C vacancies and Fe vacancies in Fe(110)–graphene system. The abbreviations: 1L, 2L, and 3L express 1 layer, 2 layers, and 3 layers, respectively.

Vacancy	E^f (eV)
C_1	1.94
C_2	1.97
Fe-v-1L	0.93
Fe-v-2L	1.87
Fe-v-3L	2.13
Fe-v-bulk	2.17

Apart from vacancies, interstitial atoms are also formed under the neutron irradiation condition. Figure 5 illustrates three different interstitial sites at the interface. The symbols, H, T, and B represent the hollow, top, and bridge position, respectively. The relative stabilities of the single interstitial C atom and Fe atom at the three sites are investigated. The interstitial Fe atom prefers to stay at the hollow site, and its formation energy is ~ 1.83 eV, which is lower than the formation energy for the tetrahedral site in bulk Fe. In addition, the interstitial atoms have a notable effect on the atomic configurations of the neighboring atoms. The interstitial Fe atom pushes the graphene layer up and affects the configuration of the Fe layers (see Fig. 6(a)). The interstitial C atom prefers to stay in the Fe layer (Fig. 6(b)), and its formation energy is 1.41 eV. These results suggest that the interstitial atoms can be easily trapped at the interface. Therefore, the interface is regarded as a sink that can trap intrinsic defects.

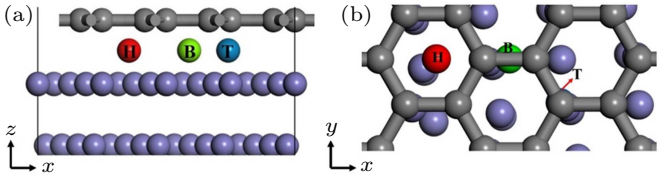


Fig. 5. Three candidate sites at Fe(110)–graphene interface (only part of atoms in an interface are displayed here for clarity), showing (a) side view and (b) top view of structure, where red, green, and blue balls represent hollow, bridge, and top sites, respectively.

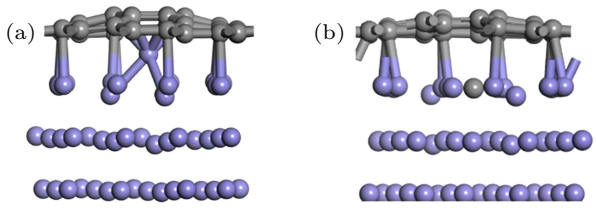


Fig. 6. (a) Structure of interstitial Fe atom and (b) structure of the interstitial C atom at Fe(110)–graphene interface, with purple and gray balls representing Fe and C atoms, respectively.

3.3. Stability and diffusion of He atoms at interface

Under long-term neutron irradiation, a certain number of He atoms can be produced by the (n, α) transmutation reaction.[58–60] Then, He bubbles can form at the interface and grain boundaries, thereby resulting in the He embrittlement of the structural material.[56,61,62] Therefore, it is critical to investigate the effects of He atoms at the interface. After optimization, it is found that the interstitial He atoms at the T and B sites are unstable and spontaneously move to the H site. Thus, an interstitial He atom prefers to stay stably at the H site and the bottom of the C_2 site, the formation energy values for an interstitial He atom at these sites are 2.09 eV and 3.07 eV, respectively. Considering the energetics, the H site is the most stable, whereas the bottom of C_2 site is a metastable for He atoms. According to Fig. 3, the H site and bottom of C_2 site have low electron density, and previous studies have shown that He atoms tend to be stable in areas with a low electron density.[62–64]

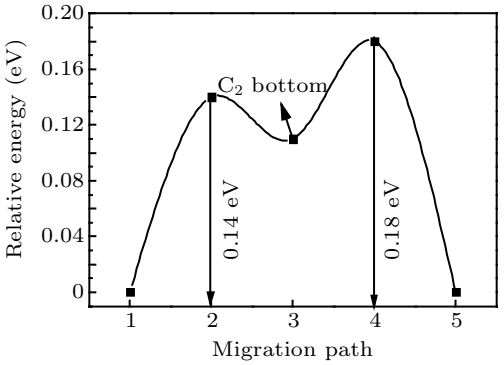


Fig. 7. Diffusion barrier profile of intersitital He atom at Fe(110)–graphene interface, indicating that He atom migrates from stable hollow site to the nearest neighboring hollow site, and diffusion path passes through another stable site of C_2 bottom.

Further, the diffusion of He atoms at the interface is vital for the formation of He bubbles. Therefore, He migration in Fe(110)–graphene is studied by the CI-NEB method. The energy for He migration between the two nearest neighbor H sites is calculated, and the result is presented in Fig. 7. The value for this process is ~ 0.18 eV. In addition, the binding energy of two He atoms at the interface is ~ 1.36 eV. The interaction between He atoms is attractive, which is the driving force for its aggregation. As the migration barrier is small and the binding energy of He atoms is relatively large, the He atoms tend to aggregate at the interface.

Graphene is impermeable to standard gases, including the He gas.[65] The He atom has a 1s closed shell electronic structure, and it does not interact chemically with graphene. Leenaerts *et al.*[66] preformed first principles calculations to investigate the penetration of He atoms through a graphene monolayer with a C vacancy. The diffusion barrier of graphene with a C vacancy is found to be ~ 18.8 eV with local density approximation (LDA) and 11.7 eV with GGA. Owing to the large migration energy, graphene can act as a barrier to impede the penetration of thermal equilibrium He at a temperature when the graphene layer remains stable. In this work, the penetration of He atoms is studied with a C vacancy in the Fe(110)–graphene system. First, a He atom is placed in vacuum far from the graphene surface to determine its stable site. After this optimization, the vertical distance between the He atom and interface is found to be ~ 2.896 Å. Then, the migration of He atoms between the comfortable site and H site is investigated, and the result is presented in Fig. 8. The migration energy is ~ 11.79 eV in this case. The high energy barrier restricts the diffusion of He across the graphene layer to reach the interface. The result illustrates that the impermeability of graphene is not reduced by the presence of Fe layers. Once some He atoms penetrate the graphene structure to reach the interface, they are trapped there and aggregated into larger species.

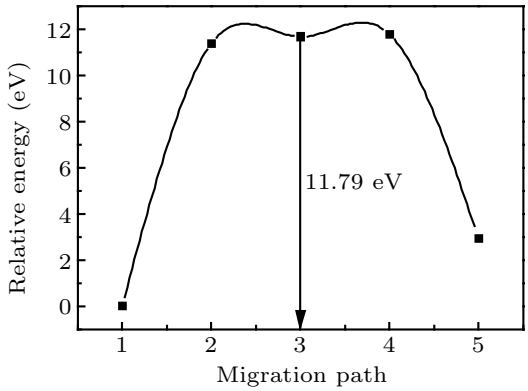


Fig. 8. Migration energy of He atom in Fe(110)–graphene system with a C vacancy: He atom migrates from vacuum to hollow site at interface though a C vacancy in graphene layer.

At the same time, the He formation energy at the tetrahedral interstitial site in the Fe substrate is 5.00 eV, larger than that at the interface. This phenomenon strongly indicates that the Fe(110)–graphene interface acts as a sink that traps He atoms. In order to study the role of graphene, we calculate the diffusion barrier of a single He atom in a structure with seven Fe layers. The migration path is shown in Fig. 9. The diffusion barrier is 7.24 eV, which is obviously lower than that for the Fe(110)–graphene system. Hence, it is concluded that the graphene acts as a buffer layer. Thus, the low formation energy and high diffusion barrier of He atoms at the interface delay the detrimental effects of He and allow the structural material to remain in service for longer.

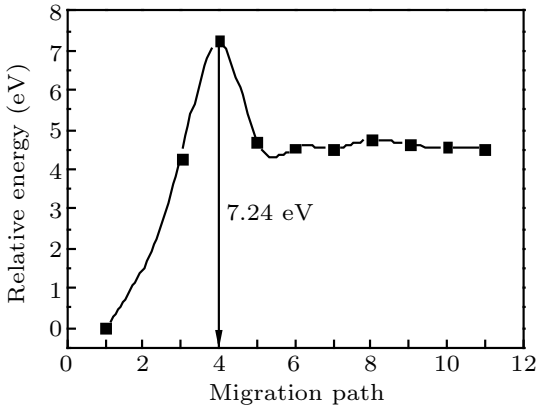


Fig. 9. Diffusion barrier of a single He atom in structure with seven Fe layers, showing that barrier between vacuum and the first Fe layer is ~ 7.24 eV.

4. Conclusions

The behaviors of point defects and He atoms are investigated via *ab initio* calculations based on DFT, and the results are compared with those of bcc Fe (bulk) and a single graphene layer. The conclusions drawn from the present study are as follows.

(i) A strong interaction and an intense Fe-3d–C-2p orbital hybridization are responsible for the stable graphene structure on the Fe(110) substrate.

(ii) Vacancies and interstitial atoms are easily formed at the interface, and the interface can act as a sink for point defects.

(iii) The He atoms require a large energy barrier to penetrate the graphene layer with a C vacancy and the binding energy of the He atoms is larger at the interface. This means that the interface impedes the diffusion of He atoms, and serves as a sink that traps the He atoms.

Acknowledgement

The authors are grateful to the Supercomputing Center of Dalian University of Technology and the Project of Nuclear Power Technology Innovation Center of Science Technology and Industry for National Defense for the computational support (Contract No. HDLCXZX-2019-ZH-28).

References

[1] Murty K L and Charit I 2008 *J. Nucl. Mater.* **383** 189
[2] Trinkaus H and Singh B 2003 *J. Nucl. Mater.* **323** 229
[3] Lucas A 1984 *Physical B + C* **127** 225
[4] Zinkle S J 2005 *Phys. Plasmas* **12** 058101
[5] Wirth B D 2007 *Science* **318** 923
[6] Arakawa K, Ono K, Isshiki M, Mimura K, Uchikoshi Mand Mori H 2007 *Science* **318** 956
[7] Bai X M, Voter A F, Hoagland R G, Nastasi M and Uberuaga B P 2010 *Science* **327** 1631
[8] Ackland G 2010 *Science* **327** 1587
[9] Xu H X, Stoller R E, Osetsky Y N and Terentyev D 2013 *Phys. Rev. Lett.* **110** 265503
[10] Dai Y Y, Ao L, Sun Q Q, Yang L, Nie J L, Peng S M, Long X G, Zhou X S, Zu X T, Liu L, Sun X, Terentyen D and Gao F 2015 *Comp. Mater. Sci.* **101** 293
[11] Heinisch H L, Gao F and Kurtz R J 2004 *J. Nucl. Mater.* **329–333** 924
[12] Zhernenkov M, Gill S, Stanic V, DiMasi E, Kisslinger K, Baldwin J K, Misra A, Demkowicz M J and Ecker L 2014 *Appl. Phys. Lett.* **104** 241906
[13] Huang H, Tang X, Chen F, Liu Jian, Sun X and Ji L 2018 *J. Nucl. Mater.* **510** 1
[14] Han W, Demkowicz MJ, Mara N A, Fu E, Sinha S, Rollett A D, Wang Y, Carpenter J S, Beyerlein I J and Misra A 2013 *Adv. Mater.* **25** 6975
[15] Gonzales C and Iglesias R 2016 *Mater. Des.* **91** 171
[16] Lach T G, Ekiz E H, Averback R S, Mara N A and Bellon P 2015 *J. Nucl. Mater.* **466** 36
[17] Chen D, Li N, Ding Y, Wen J, Baldwin K, Demkowicz M J and Wang Y 2017 *Mater. Res. Lett.* **5** 335
[18] Balandin A A, Ghosh S, Bao W Z, Calizo I, Teweldebrhan D, Miao F and Lau C N 2008 *Nano Lett.* **8** 902
[19] Balandin A A 2011 *Nat. Mater.* **10** 569
[20] Zhang C, Zhao W, Bi K, Ma J, Wang J, Ni Z, Ni Z and Chen Y 2013 *Carbon* **64** 61
[21] Huang H, Tang X, Chen F, Yang Y, Liu J, Li H and Chen D 2015 *J. Nucl. Mater.* **460** 16
[22] Huang H, Tang X, Chen F, Gao F, Peng Q and Ji L 2018 *J. Alloys Compd.* **765** 253
[23] Kim Y, Beak J, Kim S, Kim S, Ryu S, Jeon S and Han S M 2016 *Sci. Rep.* **6** 24785
[24] Ishizaki T, Xu Q, Yoshiie T, Nagata S and Troev T 2002 *J. Nucl. Mater.* **307–311** 961
[25] Katoh Y, Ando M and Kohyama A 2003 *J. Nucl. Mater.* **323** 251
[26] Stewart D, Osetskiy Y and Stoller R 2011 *J. Nucl. Mater.* **417** 1110
[27] Caro A, Hetherly J, Stukowski A, Caro M, Martinez E, Srivilliputhur S, Zepeda-Ruiz L and Nastasi M 2011 *J. Nucl. Mater.* **418** 261
[28] Abhishek A, Warrier M, Ganesh R and Caro A 2016 *J. Nucl. Mater.* **472** 82
[29] Hammond K D, Blondel S, Hu L, Maroudas D and Wirth B D 2018 *Acta Mater.* **144** 561
[30] Hohenberg P and Kohn W 1964 *Phys. Rev.* **136** B864
[31] Kohn W and Sham L J 1965 *Phys. Rev.* **140** A1133
[32] Kresse G 1995 *J. Non-cryst. Solids* **192–193** 222
[33] Kresse G and Furthmüller J 1996 *Phys. Rev. B* **54** 11169
[34] Blöchl P E 1994 *Phys. Rev. B* **50** 17953
[35] Kresse G and Joubert D 1999 *Phys. Rev. B* **59** 1758
[36] Perdew J P, Chevary J, Vosko S, Jackson K A, Pederson M R, Singh D and Fiolhais C 1992 *Phys. Rev. B* **46** 6671
[37] Perdew J P, Burke K, Ernzerhof M and Ernzerhof M 1996 *Phys. Rev. Lett.* **77** 3865
[38] Crimme S, Antony J, Ehrlich S and Krieg H 2010 *J. Chem. Phys.* **132** 154104
[39] Vinogradov N A, Zakharov A A, Kocevski V, Rusz J, Simonov K A, Eriksson O and Mikkelsen A 2012 *Phys. Rev. Lett.* **109** 026101
[40] Pei W, Zhou S, Bai Y and Zhao J 2018 *Carbon* **133** 260
[41] Khomyakov P A, Giovannetti G, Rusu P C, Brocks G, van den Brink J and Kelly P J 2009 *Phys. Rev. B* **79** 195425
[42] Dai X, Zhao J, Xie M, Tang Y, Li Y and Zhao B 2011 *Eur. Phys. J. B* **80** 343
[43] HenKelman G and Jónsson H 2000 *J. Chem. Phys.* **113** 9978
[44] Henkelman G, Uberuaga B P and Jónsson H 2000 *J. Chem. Phys.* **113** 9901
[45] Sun D, Ding J H, Huang S S, Zhang P B and Zhao J J 2018 *J. Alloys Compd.* **741** 900
[46] Batzill M 2012 *Surf. Sci. Rep.* **67** 83
[47] Liu W, Wang W, Wang J, Wang F, Lu C, Jin F, Zhang A, Zhang Q, van der Laan G, Xu Y B, Li Q X and Zhang R 2015 *Sci. Rep.* **5** 11911
[48] Cabrera M F, Baskes M I, V Melechko Anatoil and L Simpson Michael 2008 *Phys. Rev. B* **77** 035405
[49] Sutter P, Sadowski T and Sutter E 2009 *Phys. Rev. B* **80** 245411
[50] Pacilé D, Lisi S, Bernardo I D, Papagno M, Ferrari L, Pisarra M, Caputo M, Mahatha S K, Sheverdyaeva P M, Moras P, Lacovig P, Lizzit S, Baraldi A, Betti M G and Carbone C 2014 *Phys. Rev. B* **90** 195446
[51] Preobrajenski A B, Ng M L, Vinogradov A S and Martensson N 2008 *Phys. Rev. B* **78** 073401
[52] Rusz J, Preobrajenski A B, Ng M, Vinogradov A S, Martensson N and Wessely O 2010 *Phys. Rev. B* **81** 0733402
[53] Weser M, Rehder Y, Horn K, Sicot M, Fonin M, Preobrajenski A B, Voloshina E N, Goering E and Dedkov Y S 2010 *Appl. Phys. Lett.* **96** 012504
[54] Dedkov Y S and Fonin M 2010 *New J. Phys.* **12** 125004
[55] Ma B, Cong C, Wen Y, Chen R, Cho K and Shan B 2014 *J. Appl. Phys.* **115** 183708
[56] Yang T, Yang L, Liu H, Zhou H, Peng S, Zhou X, Gao F and Zu X 2017 *J. Alloys Compd.* **692** 49
[57] Adamska L, Lin Y, Ross A J, Batzill M and Oleynik I I 2012 *Phys. Rev. B* **85** 195443
[58] Duffy D 2010 *Phil. Trans. R. Soc A* **368** 3315
[59] Stoller R E 1990 *J. Nucl. Mater.* **174** 289
[60] Hsiung L L, Fluss M J, Tumey S J, Choi B W, Serruys Y, Willaime F and Kimura A 2010 *Phys. Rev. B* **82** 184103
[61] Gilbert M R, Dudarev S L, Manh D N, Zheng S, Packer L W and Sublet J C 2013 *J. Nucl. Mater.* **442** S755
[62] Puska M J, Nieminen R M and Manninen M 1981 *Phys. Rev. B* **24** 3037
[63] Sen H S and Polcar T 2019 *J. Nucl. Mater.* **518** 11
[64] Saikia U, Sahariah M B, González C and Pandey R 2018 *Sci. Rep.* **8** 3844
[65] Scott Bunch J, Verbridge S S, Aiden J S, van der Zande A M, Parpia J M, Craighead H G and McEuen P L 2008 *Nano Lett.* **8** 2458
[66] Leenaerts O, Partoens B and Peeters F M 2008 *Appl. Phys. Lett.* **93** 193107